Electronic Supplementary Material (ESI) for ChemComm.

Supporting Information

Cancer Cell-Targeted Nanoprobe for Multilayer Imaging of Diverse Biomarkers and Precise Photodynamic Therapy

Zhuolin Fu [a], Yingdi Wu [a], Chunnian Ren [b], Weiling Song [a], Xiaoru Zhang [a], Meie Yue [a] and Ying Li*[a]

[a]Key Laboratory of Optic-electric Sensing and Analytical Chemistry for Life Science, MOE; Shandong Key Laboratory of Biochemical Analysis; Key Laboratory of Analytical Chemistry for Life Science in Universities of Shandong; College of Chemistry and Molecular Engineering. Qingdao University of Science and Technology, Qingdao 266042, PR China.

[b]College of Information Science and Technology, Qingdao University of Science and Technology, Qingdao, 266042, PR China

S1 Experimental section

S1.1 Materials and Reagents

The oligonucleotides used in this experiment were synthesized by Sangon Biotech Co., Ltd. (Shanghai, China) and their sequences are listed in Table S1. Chloroauric acid ($HAuCl_4 \cdot 3H_2O$) and sodium citrate ($Na_3C_6H_5O_7 \cdot 2H_2O$) were ordered from Sigma-Aldrich (St. Louis, MO). Roswell Park Memorial Institute (RPMI)-1640 medium and Dulbecco's Modified Eagle Medium (DMEM) were purchased from Wolcavi (Beijing) biotechnology Co., Ltd. Annexin V-FITC/PI Apoptosis Detection Kit and Cell counting kit-8 (CCK-8) were obtained from Sangon Biotech Co. Ltd. (Shanghai, China). 1,3-diphenyl isobenzofuran (DPBF) was purchased from Shanghai Macklin Bionchemical Co., Ltd. Annexin V-FITC-PI Apoptosis Detection Kit was purchased from Vazyme biotech. Co., Ltd. Reactive xygen species (ROS) assay kit was purchased from G-CLONE Biotech Co. Ltd. (Beijing, China). The cells were obtained from Tumor Marker Research Center, Cancer Hospital of the Chinese Academy of Medical Sciences (Beijing, China). Other chemicals employed were of analytical reagent grade and were used without further purification.

Table S1. DNA Sequence Used in This Work

Oligonucleotides name	Sequences	Description
Rox-H	5’-Rox-TCAACATCAGTCTGACCAAAGGATC AACTGCAGACACT-SH-3’	Rox labled hairpin DNA
Cy3-A	5’-Cy3-GCAGTTGATCCTTTGGATACCCTGG-3’	Cy3 modified MUC1-specific aptamer
Ce6-S	5'-Ce6-CCCATTCCCATTCCCATTCC-SH-3'	Ce6 labled single-strand DNA
miRNA-21	5′-UAGCUUAUCAGACUGAUGUUGA-3′	the target miRNA

The structure of Rox

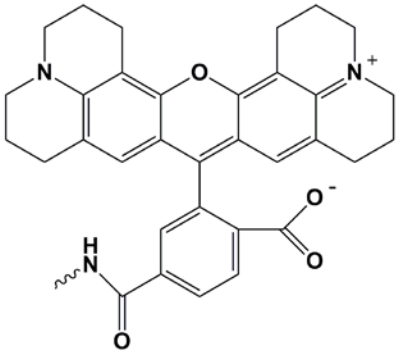

The structure of Cy3

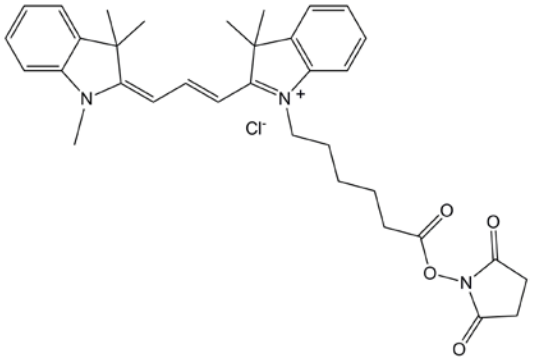

S1.2 Apparatus

Transmission electron microscopy (TEM) images were taken with a JEM F2100 Field Emission Transmission Electron Microscope (JEOL). UV-vis absorption spectra were obtained with a Cary 50 UV/vis-NIR spectrophotometer (Varian, USA). Dynamic light scattering (DLS) were measured by Zetasizer Nano ZS (Malvern, U.K.). SERS detection was performed on an inVia Raman microscope (Renishaw, England). Fluorescence imaging was performed using a Leica TCS SP5 inverted confocal microscope (Leica, Germany). Flow cytometry analysis was performed using CytoFLEX flow cytometer (Beckman Coulter Commercial Enterprise Co. Ltd). CCK-8 assay was determined by a microplate reader (Bio-Tek, America), the absorbance at 450 nm was recorded.

S1.3 Preparation of AuNPs

Au nanoparticles (AuNPs) were synthesized according to the traditional citrate reduction method. [1] Before using the distilling flask and the condenser pipe were immersed in the nitric acid solution for one day and then rinsed by deionized water. 100 mL of 0.01% $HAuCl_4$ solution was added to the distilling flask and stirred continuously with heat treatment to reach its boiling point. Then 1.5 mL of 1% trisodium citrate solution was added and the color of the solution was changed from a primrose yellow to a wine red. After refluxing for another 30 min the AuNPs solution was cooled to room temperature and the obtained gold colloidal solutions were stored in brown bottle at 4 °C temperature for the follwing experiments.

S1.4 Preparation of the multifunctional nanoprobe

Before using 50.0 μL of 1.0 μM DNA **ROX-H** (3'-thiol and 5'-Rox) was annealed at 95 °C water bath for 5 min and cooled with ice bath. For preparing the multifunctional nanoprobe, the annealed DNA **ROX-H** was mixed with 3'-thiol and 5'-Ce6 modified DNA **Ce6-S** (1.0 μM, 50.0 μL) and the mixture was then added to 1 mL of AuNPs. After shaking gently in the oscillator for about 16 h at 37 °C, 200.0 μL of 0.05 M NaCl was blended with the mixture and aged for 6 h. Then 200.0 μL of 0.1 M NaCl was added and aged for another 6 h. DNA **ROX-H** and **Ce6-S** were immobilized on the surfaces of AuNPs via covalent gold-thiol bonds. Subsequently, the mixture were centrifuged at 12000 rpm for 30 min to remove the excess sequence and resuspended in 5'-Cy3 modified DNA **Cy3-A** (1 μM, 50 μL) for 2 h. The prepared multifunctional probe was

determined by measuring the Raman signals of Rox and Cy3 and then stored at 4 ℃ in the refrigerator for subsequent experiments.

S1.5 SERS characterization of the probe

1.5 μL of the prepared probe was casted onto the surface of gold film and air-dried at room temperature. The Raman spectra were measured at 633 nm excitation laser with 50×objective lens (laser power of 5 mW, and the acquisition time of each spectrum was 5 s).

S1.6 Cell culture

MCF-7, HEK293T and HepG2 cells were employed in this experiment. MCF-7 and HepG2 cells were cultured in RPMI 1640 medium containing heat-inactivated bovine serum (10%) and penicillin-streptomycin (1%). HEK293T cells were cultured in Dulbecco's Modified Eagle's Medium (DMEM) supplemented with heat-inactivated bovine serum (10%). The cells were grown in 25 cm^2 cell culture flasks at 37 °C in a humidified atmosphere (5% CO_2 and 95% air).

S1.7 Fluorescence microscopy analysis of the living cells

MCF-7 and HEK293T cells were cultured in confocal dishes for 24 h and 15 μL of the prepared multifunctional nanoprobe was then added to the cells. After incubating for some time, the extracellular probes were removed by washing the cells with PBS solution for three times for reducing the background fluorescence. By utilizing a 40× objective, the cells were imagined with the confocal laser scanning microscope and the excitation source was 514 nm. The fluorescence emission of Cy3 and Rox was collected from 560-600 and 600-640 nm of band-pass filter respectively.

S1.8 Evaluation of ROS generation in solution

1,3-diphenyl isobenzofuran (DPBF) was used to evaluate the singlet oxygen production ability of the nanoprobe. DPBF can be oxidized by singlet oxygen and loses the absorption at about 410 nm. Briefly, the mixed solution of DPBF and the nanoprobe was irradiated under 650 nm laser for different time and the absorption intensity of DPBF at 410 nm was recorded.

S1.9 Evaluation of intracellular ROS generation

The intracellular $^1O_2$ generation inside cells was detected using 2,7'-dichlorodihydrofluorescein diacetate (DCFH-DA). The MCF-7 cells were seeded in culture dish for 24 h at 37 °C. Then the medium was removed and the multifunctional nanoprobe was added. After incubating for 4 h, the cells were washed twice with PBS and further incubated with 10 μM DCFH-DA for 30 min. After washing, the cells were irradiated by a 650 nm laser for 15 min with the power intensity of 10 $mW•cm^{-2}$. Finally, the cells were imaged under a confocal laser scanning microscope with the excitation laser at 488 nm and collected emission wavelength from 500 to 520 nm. The cells treated without the nanoprobe were used as the control.

S1.10 Cell Viability Assay

MCF-7 cells, HEK293T cells (human renal epithelial cells), and HepG2 cells (MUC1-negative liver hepatocellular cells) were seeded into 96-well plates and cultured at 37 °C in 5% CO_2 atmosphere for 24 h. After incubating with different concentrations of AuNPs or the multifunctional nanoprobe for 4 h, the cells were washed with PBS and irradiated at 650 nm for 30 min. The cell without laser irradiation

were used as the control. Subsequently, 10 μL of CCK-8 solution was added into each well, and the cells were further incubated for 4 h. Afterward, the optical density (OD) at 450 nm of each well were measured on a microplate reader. Cell viability was calculated as described by the manufacturer.

S1.11 Apoptosis Assay

Using Annexin V-FITC apoptosis detection kit flow cytometry evaluation of cell apoptosis induced by PDT were detected. After incubating with the multifunctional nanoprobe for 4 h, the MCF-7 cells were irradiated by a 650 nm laser for 20 min with the power intensity of 10 $mW•cm^{-2}$. Then the cells were digested using trypsin and collected by centrifugation. Followed by resuspending in 100 μL binding buffer, 5 μL of Annexin V-FITC and 10 μL of PI were added and the cells were incubated for 15 min at room temperature. Finally, the apoptosis of different cell amples were respectively analyzed by flow cytometer.

S2 Results and Discussion

S2.1 Characterization of gold nanoparticles (AuNPs)

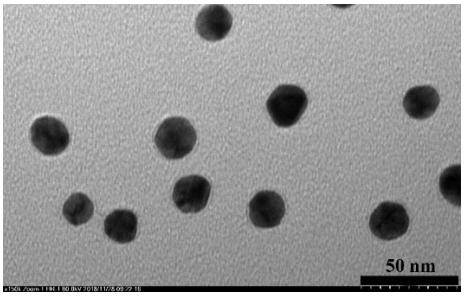

Fig. S1. TEM image of the synthesised AuNPs

S2.2 UV-visible characterization of the prepared nanoprobe

The UV-visible spectra of AuNPs, Cy3-A, Rox-H and the prepared nanoprobe were measured through a Cary 50 UV/Vis-NIR spectrophotometer. As described in Fig. S2 ,

curve a, b and c exhibited the characteristic absorption peak of AuNPs (~520 nm), Cy3-A (~260 nm and a characteristic absorbance at 520~620 nm), Rox-H (~260 nm and 520~620 nm). Curve d exhibited the characteristic absorbance of AuNPs, Cy3-A, and Rox-H, which indicated that Cy3-A, and Rox-H had successfully conjugated with the AuNPs.

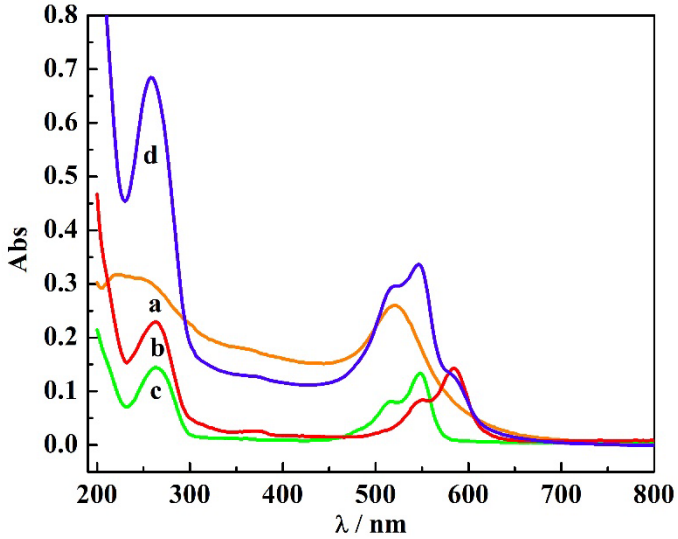

Fig. S2. UV spectra of (a) AuNPs, (b) Cy3-A, (c) Rox-H and (d) the prepared nanoprobe

S2.3 DLS characterization of the nanoprobe

The hydrodynamic diameter and zeta potential of nanoprobe were analyzed by Dynamic Light Scattering (DLS). As shown in Fig. S3A, the average hydrodynamic diameter of AuNPs were 43 nm, and the average size increased to 58 nm after surface modified of AuNPs with DNA. From Fig. S3B it could be seen that the zeta potential of the nanoprobe was more negative than AuNPs due to the negatively charged DNA modified on the surface of AuNPs. The results can also demonstrate the successful preparation of the nanoprobe.

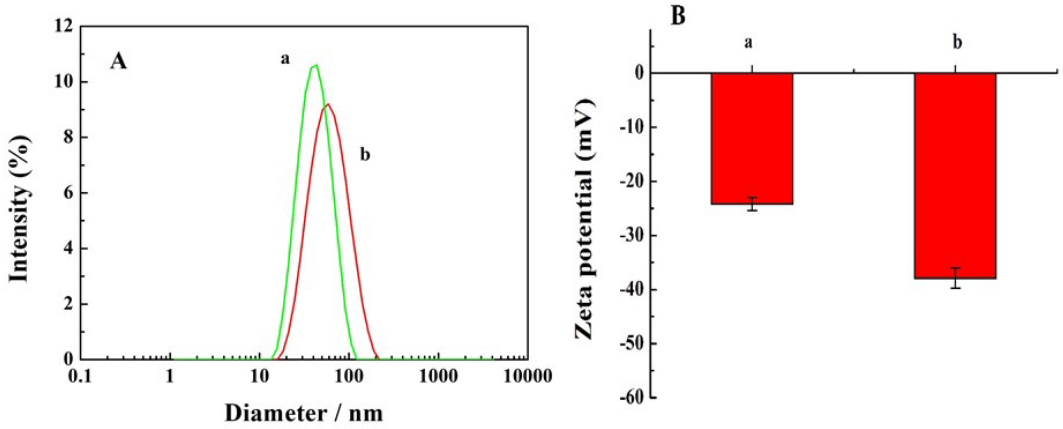

Fig. S3. (A) DLS spectra of (a) AuNPs, (b) nanoprobe, (B) ζ-potential measurements of (a) AuNPs, (b) nanoprobe

S2.4 Stability of the prepared nanoprobe

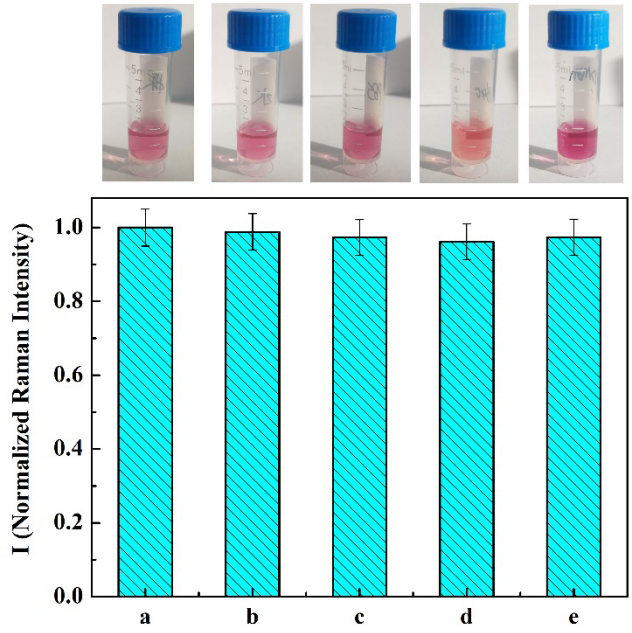

Fig. S4 The images of the prepared nanoprobe dispersed in PBS for 0 h (a) and those dispersed in PBS (b), H_2O (c), RPMI-1640 (d), DMEM (e) for 48 h. The column graph is the Raman intensity of Cy3 at 1586 cm^{-1}.

The stability of the nanoprobe was studied by dispersing the probe in four media including H_2O, PBS, RPMI-1640 and DMEM. The changes were observed after being stored for 48 h at room temperature. As shown in Fig. S4, no turbidity and precipitation

were observed in four media. The Raman spectra of the nanoprobe were then recorded and the comparision result was also shown in Fig. S4. No obvious change was found, indicating that the nanoprobe has good dispersibility and stability.

S2.5 Specificy imaging of MCF-7 and HepG2 cells

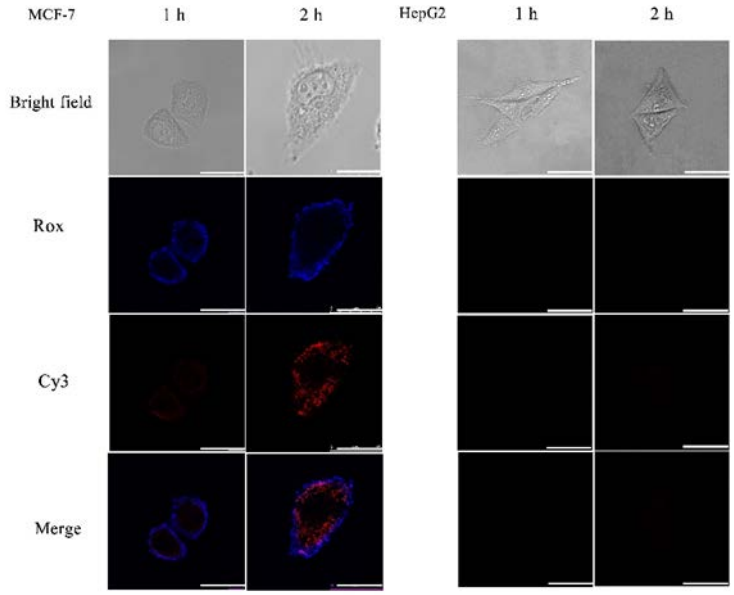

Fig. S5. Fluorescence confocal images of MCF-7 and HepG2 cells after incubation with the nanoprobes for 1 h and 2 h. Scale bars: 25 μm.

S2.6 ROS generation in solution

For evaluating the ROS generation in solution, DPBF was used and the results were shown in Fig. S5. From Fig. S5A it could be seen that in the presence of the nanoprobe the absorption intensity of DPBF at 410 nm gradually decreased with the extension of irradiation time. However, the absorption intensity of DPBF and the mixture of DPBF-nanoprobe without laser irradiation (Fig. S5B, curve a and b) did not decrease at 410 nm. Meanwhile, the absorption intensity of DPBF with laser irradiation (Fig. S5B, curve c) did not decrease either. These results indicate that the nanoprobe has efficient

photodynamic activities for $^1O_2$ generation under the 650 nm laser irradiation.

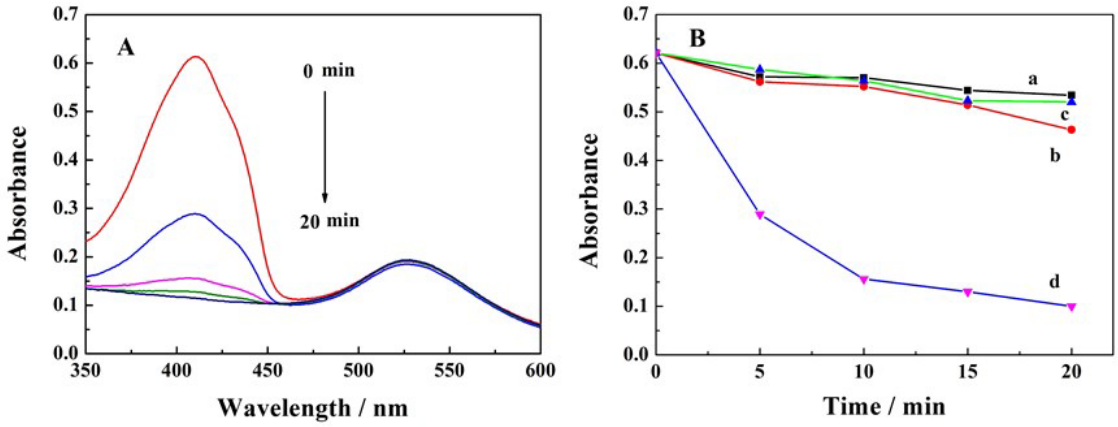

Fig. S6. (A) UV spectra of DPBF-nanoprobe with different irradiation time. (B) The changes of the absorbance at 410 nm with different treatments: (a) DPBF, (b) DPBF with irradiation, (c) DPBF -nanoprobe, (d) DPBF-nanoprobe with laser irradiation.

S2.7 Comparison between the proposed method and other reported approaches for targeted-cancer cell imaging and therapy

Table S2. Comparison between the proposed method and other reported approaches for targeted-cancer cell imaging and therapy

Tybe of the probe	Target expressed by cancer cell	Number of biomarkers	Multilayer imaging	Tumor therapy	Reference
MoS_2 quantum dots	MUC1	1	No	No	2
Titanium Carbide MXenes	MUC1	2	Yes	No	3
DNA tetrahedron	MUC1	1	No	Yes	4
Dox-loaded nanoprobe	MUC1	2	Yes	Yes	5
Magnetic RNA Nanoflowers	Folate receptor	1	No	Yes	6

Dox-loaded nanoprobe	Nucleolin	2	Yes	Yes	7
Dox-loaded exosome	PTK7	1	No	Yes	8
Ce6-modified multifunctional nanoprobe	MUC1	2	Yes	Yes	This work

S2.8 Apoptotic population comparison between the proposed method and other reported approaches

Table S3. Apoptotic population comparison between the proposed method and other reported approaches

Type of photosensitizer	Apoptotic population of Flow cytometric analysis	Reference
Porphyrin	25.79%	9
Ce6	40.6%	10
Graphitic carbon nitride	25.45%	11
Ce6	27.19%	12
Manganese phthaleincyanide	37.87%	13
Ce6	32.64%	14
Ce6	24.03%	15
Ce6	26.88%	This work

References

1 K. C .Grabar, P. C. Smith, M. D. Musick, J. A. Davis, D. G. Walter, M. A. Jackson, A. P. Guthrie, M. J. Natan, *J. Am. Chem. Soc.* 1996, **118**, 1148−1153.

2 Y. H. Liu, J. Z. Zhang, Y. S, J. D. Yan, Z. Y. Hou, C. Mao and W. B. Zhao, *RSC. Advances*., 2017, **7**, 54638−54643.

3 S. Wang, S. H. Wei, S. G. Wang, X. H. Zhu, C. Y. Lei, Y. Huang, Z. Nie and S. Z. Yao, *Anal Chem*., 2019, **91**, 1651−1658.

4 X. Han, Y. J. Jiang, S. Y. Li, Y. Zhang, X. N. Ma, Z. H. Wu, Z. H. Wu and X. L. Qi, *Nanoscale*, 2019, **11**, 339−347.

5 H. B. Si, L. J. Wang, Q. L. Li, X. X. Li, L. Li and B. Tang, *Chem. Commun*., 2018, **54**, 8277−8280.

6 Y. S. Guo, S. Li, Y. J. Wang and S. S. Zhang, *Anal. Chem.*, 2017, **89**, 2267−2274.

7 X. T. Liu, L. Wang, X. W. Xu, H. Y. Zhao and W. Jiang, *ACS Appl. Mater. Interfaces*., 2018, **10**, 39524−39531..

8 J. M. Zou, M. L. Shi, X. J. Liu, C. Jin, X. J Xing, L. P. Qiu and W. H. Tan, *Anal. Chem*., 2019, **91**, 2425−2430

9 M. Pan, Q. Y Jiang, J. L. Sun, Z. Xu, Y. Z. Zhou, L. Zhang and X. Q. Liu, *Angew. Chem. Int. Ed. Engl*., 2020, **59**, 1897−1905.

10 D. Q. Wang, N. Zhang, X. N. Jing, Y. Zhang, Y. Z. Xu and L. J. Meng, *J. Mater. Chem. B*., 2020, **8**, 8271−8281.

11 J. Y. Dai, J. B. Song, Y. Qiu, J. J. Wei, Z. Z. Hong, L. Li and H. H. Yang, *ACS. Appl. Mater. Interfaces*., 2019, **11**, 10589−10596.

12 N. Li, M. H. Xiang, J. W. Liu, H. Tang and J. H. Jiang, *Anal. Chem*., 2018, **90 (21)**, 12951−12958.

13 Y. Zhu, H. D. Shi, T. W. Li, J. J. Yu, Z. X. Guo, J. J. Cheng and Y. Z. Liu, *ACS. Appl. Mater. Interfaces*., 2020, **12**, 18309−18318.

14 D. Zhang, M. Wu, Y. Y. Zeng, L. J. Wu, Q. T. Wang, X. Han, X. L. Liu and J. F. Liu, *ACS. Appl. Mater. Interfaces*., 2015, **7**, 8176−87.

15 Z. X. Xie, S. Liang, X. C. Cai, B. B. Ding, S. S. Huang, Z. Y. Hou, P. A. Ma, Z. Y. Cheng and J. Lin, *ACS. Appl. Mater. Interfaces*., 2019, **11**, 31671−31680.